

DUST PRODUCTION FACTORIES IN THE EARLY UNIVERSE: FORMATION OF CARBON GRAINS IN RED-SUPERGIANT WINDS OF VERY MASSIVE POPULATION III STARS

TAKAYA NOZAWA^{1,2}, SUNG-CHUL YOON³, KEIICHI MAEDA^{4,2}, TAKASHI KOZASA⁵
KEN'ICHI NOMOTO^{2,7}, AND NORBERT LANGER⁶

accepted on 20 April 2014

ABSTRACT

We investigate the formation of dust in a stellar wind during the red-supergiant (RSG) phase of a very massive Population III star with the zero-age main sequence mass of $500 M_{\odot}$. We show that, in a carbon-rich wind with a constant velocity, carbon grains can form with a lognormal-like size distribution, and that all of the carbon available for dust formation finally condense into dust for wide ranges of the mass-loss rate ($(0.1\text{--}3)\times 10^{-3} M_{\odot} \text{ yr}^{-1}$) and wind velocity ($1\text{--}100 \text{ km s}^{-1}$). We also find that the acceleration of the wind driven by newly formed dust suppresses the grain growth but still allows more than half of gas-phase carbon to be finally locked up in dust grains. These results indicate that at most $1.7 M_{\odot}$ of carbon grains can form in total during the RSG phase of $500 M_{\odot}$ Population III stars. Such a high dust yield could place very massive primordial stars as important sources of dust at the very early epoch of the universe if the initial mass function of Population III stars was top-heavy. We also briefly discuss a new formation scenario of carbon-rich ultra-metal-poor stars considering the feedback from very massive Population III stars.

Subject headings: dust, extinction – galaxies: high-redshift – stars: massive – stars: Population III – stars: winds, outflows – supergiants

1. INTRODUCTION

The discoveries of huge amounts of dust grains in high-redshift quasars (Bertoldi et al. 2003; Priddey et al. 2003) have posed the fundamental problems on the origin of dust in the early universe. At such an early epoch, core-collapse supernovae (CCSNe) arising from massive stars are considered to be the most promising sources of dust (e.g., Dwek et al. 2007). On the other hand, the contribution from asymptotic giant branch stars evolving from intermediate-mass ($M_{\text{ZAMS}} \simeq 3\text{--}8 M_{\odot}$) stars has also been invoked to explain a large content of dust in high-redshift objects (Valiante et al. 2009; Dwek & Cherchneff 2011). What stellar mass range can mainly contribute to the dust budget in the early universe strongly depends on the initial mass function (IMF) of the stars (Valiante et al. 2011; Gall et al. 2011a, 2011b).

Numerical simulations of the formation of metal-free stars have shown that the IMF of the first generation of stars, so-called Population III (Pop III) stars, would be weighted towards much higher mass than those in the present universe (Bromm & Larson 2004; Hirano et al. 2014). However, a characteristic mass of Pop III stars remains to be clarified, spanning from $\sim 40 M_{\odot}$ (Hosokawa et al. 2011; Susa 2013) up to more than $300 M_{\odot}$ (Omukai

& Palla 2003; Ohkubo et al. 2009). In particular, Pop III stars with the masses exceeding $\sim 250 M_{\odot}$ emit numerous ionizing photons and finally collapse into black holes (BHs), serving as seeds of supermassive BHs. Thus, such very massive Pop III stars would have crucial impacts on the reionization of the universe and dynamical evolution of galaxies.

Even though most of very massive Pop III stars are not supposed to explode as supernovae (SNe), they are likely to play an important role in the chemical enrichment of the early universe. Yoon et al. (2012) found that non-rotating models with $M_{\text{ZAMS}} > 250 M_{\odot}$ undergo convective dredge-up of large amounts of carbon and oxygen from the helium-burning core to the hydrogen-rich envelope during the red-supergiant (RSG) phase. This may lead to enrichment of the surrounding medium with CNO elements via RSG winds. More importantly, such CNO-enriched RSG winds can serve as formation sites of dust in the early universe. In this Letter, we elaborate this new scenario of dust formation by Pop III stars, using an exemplary model with $M_{\text{ZAMS}} = 500 M_{\odot}$. We show that C grains can form efficiently in the stellar wind with a constant velocity for a reasonable range of mass-loss rates and wind velocities. We also discuss the effect of the wind acceleration on dust formation.

2. THE MODEL

For the properties of a $500 M_{\odot}$ RSG, we refer to the model sequence m500vk00 without rotation in Yoon et al. (2012); the average luminosity and effective temperature of this RSG are $L_{*} = 10^{7.2} L_{\odot}$ and $T_{*} = 4,440 \text{ K}$, respectively, with a stellar radius of $R_{*} = 6,750 R_{\odot}$. This very massive RSG undergoes convective dredge-up during helium-core burning, enriching the hydrogen envelope with a large amount of carbon and oxygen; the average number fractions of the major elements in the envelope are $A_{\text{H}} = 0.701$, $A_{\text{He}} = 0.294$, $A_{\text{C}} = 3.11 \times 10^{-3}$, and

¹ National Astronomical Observatory of Japan, Mitaka, Tokyo 181-8588, Japan; takaya.nozawa@nao.ac.jp

² Kavli Institute for the Physics and Mathematics of the Universe (WPI), The University of Tokyo, Kashiwa, Chiba 277-8583, Japan

³ Department of Physics and Astronomy, Seoul National University, Seoul 151-747, Korea

⁴ Department of Astronomy, Kyoto University, Sakyo-ku, Kyoto 606-8502, Japan

⁵ Department of CosmoSciences, Graduate School of Science, Hokkaido University, Sapporo 060-0810, Japan

⁶ Argelander-Institut für Astronomie der Universität Bonn, Aufdem Hügel, 53121 Bonn, Germany

⁷ Hamamatsu Professor

TABLE 1
CHEMICAL REACTIONS FOR FORMATION OF C CLUSTERS CONSIDERED IN THIS PAPER

	key molecule	chemical reaction	$A/10^4\text{K}$	B	a_0 (Å)	σ (erg cm $^{-2}$)
(1) Model A	C	$\text{C}_{n-1} + \text{C} \rightleftharpoons \text{C}_n \quad (n \geq 2)$	8.3715	22.1509	1.281	1400
(2) Model B	C_2H	$2(\text{C}_2\text{H} + \text{H}) \rightleftharpoons \text{C}_{2n} + 2\text{H}_2 \quad (n = 2)$ $\text{C}_{2(n-1)} + \text{C}_2\text{H} + \text{H} \rightleftharpoons \text{C}_{2n} + \text{H}_2 \quad (n \geq 3)$	8.6425	18.9884	1.614	1400

NOTE. — The key molecule is defined as the gas species whose collisional frequency is the least among the reactants. The Gibbs free energy $\Delta\hat{g}$ for the formation of the condensate from reactants per key molecule is approximated by $\Delta\hat{g}/kT = -A/T + B$ with the numerical values A and B derived by least-squares fittings of the thermodynamics data (Chase et al. 1985). The radius of the condensate per key molecule and the surface tension of bulk grains are a_0 and σ , respectively.

$A_{\text{O}} = 1.75 \times 10^{-3}$, leading to a high C/O ratio (C/O = 1.78).

2.1. Hydrodynamic Model of the Outflowing Gas

As the first step to assess the possibility of dust formation in a Pop III RSG wind, we consider a spherically symmetric gas flow with a constant wind velocity. In this case, the density profile of the gas flow is given by

$$\rho(r) = \frac{\dot{M}}{4\pi r^2 v_w} = \rho_* \left(\frac{r}{R_*} \right)^{-2}, \quad (1)$$

where \dot{M} is the mass-loss rate, v_w is the wind velocity, and r is the distance from the center of the star. The radial profile of the gas temperature is assumed to be

$$T(r) = T_* \left(\frac{r}{R_*} \right)^{-\frac{1}{2}}, \quad (2)$$

following the previous studies on dust formation in stellar winds (e.g., Gail et al. 1984).

Mass loss from a RSG was not considered in Yoon et al. (2012), and both the mass-loss rate and the wind velocity are hardly known for Pop III RSGs. Given that the underlying physics of mass-loss mechanisms is not well understood, modeling elaborately the mass-loss history is beyond the scope of this letter. Instead, to cover various physical conditions of the mass-loss winds, we treat \dot{M} and v_w as free parameters and examine how these quantities affect the formation process of dust. In what follows, we take as fiducial values $v_w = 20$ km s $^{-1}$ and $\dot{M} = 3 \times 10^{-3} M_{\odot} \text{ yr}^{-1}$; the latter corresponds to the constant mass-loss rate with which the $500 M_{\odot}$ star loses 90% ($208 M_{\odot}$) of the envelope during the last 7×10^4 yr of the RSG phase.⁸

2.2. Model of Dust Formation

The calculations of dust formation are performed by applying the formulation of non-steady-state dust formation in Nozawa & Kozasa (2013). The formulae self-consistently follow the formation of small clusters and the growth of grains under the consideration that the collisions of key molecules, defined as the gas species with

the least collisional frequency among the reactants, control the kinetics of dust formation process. The formulae enable us to evaluate the size distribution and condensation efficiency of newly formed grains for given temporal evolutions of gas temperature and density, chemical composition of the gas, and chemical reactions for the formation of clusters.

In a carbon-rich cool gas, all oxygen atoms are bound to carbon atoms to form CO molecules, and carbon atoms and/or carbon-bearing molecules left after the CO formation can participate in the formation of C clusters and grains. The chemical equilibrium calculations along the gas flow (e.g., Kozasa et al. 1996) show that, for the physical and chemical conditions given above, the major carbon-bearing gas species, other than CO, is atomic carbon at $T \gtrsim 1,750$ K and C_2H at $T \simeq 1,400$ – $1,700$ K. Thus, the formation of C clusters is expected to proceed at high temperatures through successive attachment of carbon atoms as given in the reaction (1) of Table 1, which we call Model A. Independently of this, we consider another dust formation path involving C_2H , for which the possible chemical reactions are given under (2) of Table 1, hereafter referred to as Model B.

In the calculations, we assume that a fraction f_{C} of the carbon that is not locked up in CO molecules exists as carbon atoms in Model A and as C_2H molecules in Model B. Since f_{C} linearly changes the number density of carbon available for dust formation, decreasing f_{C} is identical with reducing the mass-loss rate or the C/O ratio in the envelope by the same factor. The time evolutions of the gas density and temperature are calculated by substituting $r = R_* + v_w t$ into Equations (1) and (2). The sticking probability of gas species is assumed to be unity, and C clusters that contain more carbon atoms than $n_* = 100$ are treated as bulk grains. We refer the readers to Nozawa & Kozasa (2013) for the formulation of dust formation process and the detailed prescription of the calculations.

3. RESULTS OF DUST FORMATION CALCULATIONS

Figure 1 shows the results of the calculations for the fiducial case with $f_{\text{C}}\dot{M} = 3 \times 10^{-3} M_{\odot} \text{ yr}^{-1}$ and $v_w = 20$ km s $^{-1}$; Figure 1(a) plots the formation rate of seed clusters with $n_* = 100$ divided by the concentration of key species without depletion due to cluster/grain formation (I_*), condensation efficiency (f_{con}), and average grain radius (a_{ave}) as a function of distance from the center of the star (r/R_*). Here, the condensation efficiency $f_{\text{con}}(t)$ is defined as the fraction of free carbon atoms that are locked up in grains. In Model A (thick lines) and Model

⁸ We note that, even if there were no wind, floating-off of the loosely bound RSG envelope as a result of the collapse of the core into a BH at the end of its life may also lead to mass ejection of CNO elements into the interstellar medium and production of dust grains (Zhang et al. 2008; Kochanek 2014).

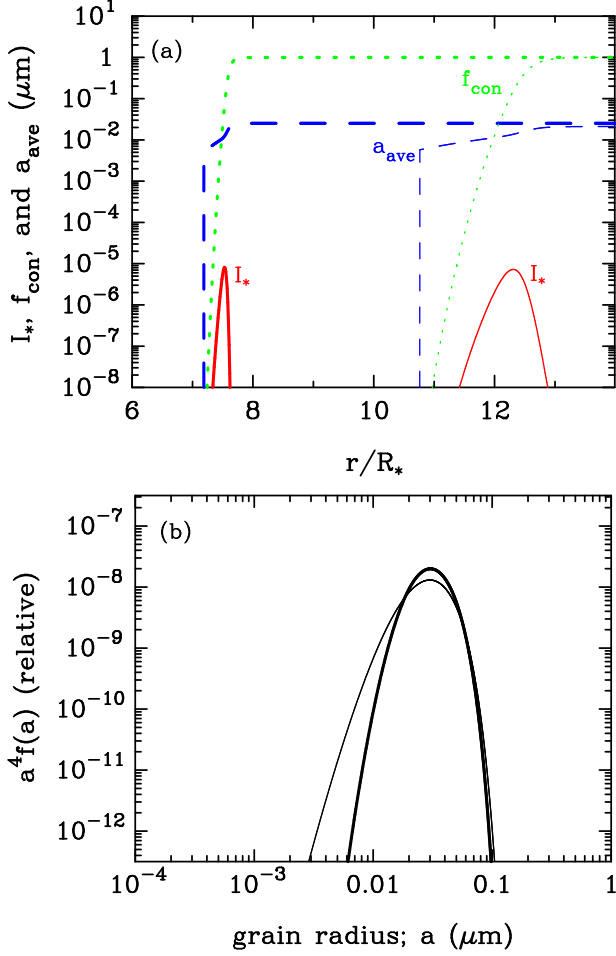


FIG. 1.— (a) Formation rate of seed clusters with $n_* = 100$, divided by the nominal concentration of the key molecules (I_* , solid), condensation efficiency (f_{con} , dotted), and average grain radius (a_{ave} , dashed) as a function of distance from the center of the star (r/R_*), and (b) final size distribution spectrum by mass $a^4 f(a)$ of newly formed C grains for a mass-loss rate $\dot{M} = 3 \times 10^{-3} M_\odot \text{ yr}^{-1}$, a wind velocity $v_w = 20 \text{ km s}^{-1}$, and $f_C = 1$. The thick lines are for the Model A where the chemical reaction (1) in Table 1 is considered for the formation of clusters, while the thin lines are for the Model B with the chemical reactions (2).

B (thin lines), dust grains start to form at $7.2 R_*$ and $10.8 R_*$, respectively, with I_* being peaked around $7.5 R_*$ and $12.3 R_*$. In both of the models, the final condensation efficiency $f_{\text{con},\infty} = f_{\text{con}}(t \rightarrow \infty)$ is unity.

The final average grain radius is only a little higher for Model A ($a_{\text{ave},\infty} = 0.025 \mu\text{m}$) than for Model B ($a_{\text{ave},\infty} = 0.021 \mu\text{m}$); for Model B, the concentration of key molecules at the time of dust formation is lower than for Model A by a factor of $\simeq 5$, but the resulting decrease in the formation rate of seed clusters is compensated with the decrease in the growth rate. As a result, the final average radius is similar in both Model A and Model B, although lower rates (longer timescales) of both processes for Model B lead to a broader lognormal-like size distribution of grains, as seen from Figure 1(b). These results demonstrate that the final condensation efficiency and average grain radius are almost independent of the chemical reactions for the formation of C clusters in the context of this study.

Figure 2(a) indicates the final condensation efficiency

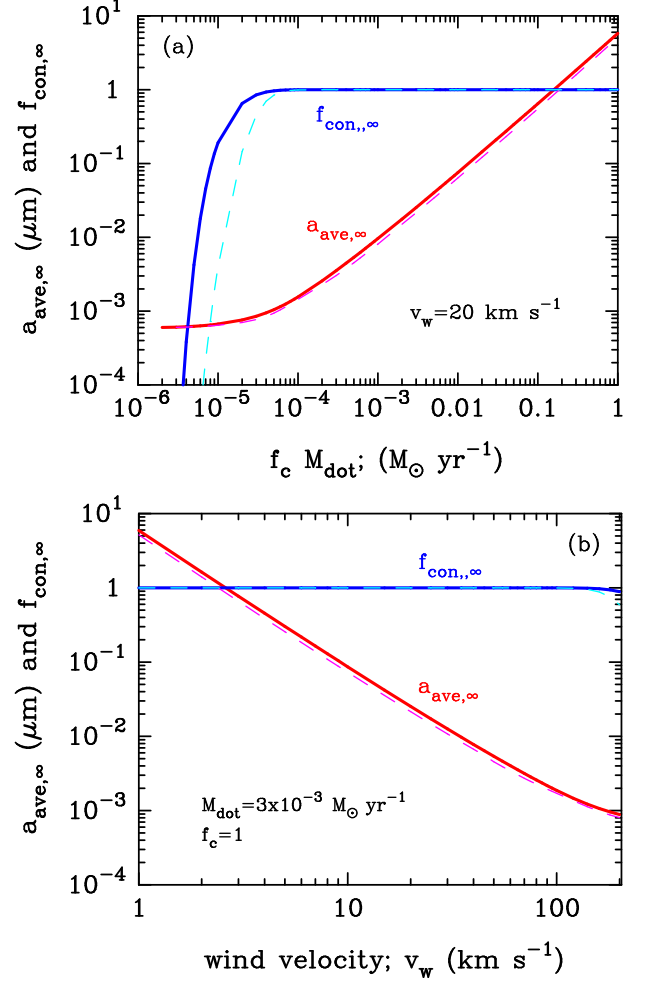


FIG. 2.— Final average radius $a_{\text{ave},\infty}$ and final condensation efficiency $f_{\text{con},\infty}$ of C grains formed in the outflowing gas; (a) as a function of product $f_C \dot{M}$ for $v_w = 20 \text{ km s}^{-1}$, and (b) as a function of v_w for $f_C \dot{M} = 3 \times 10^{-3} M_\odot \text{ yr}^{-1}$. The thick solid lines are for Model A, while the thin dashed lines are for Model B.

and final average radius of newly formed C grains as a function of product $f_C \dot{M}$ for $v_w = 20 \text{ km s}^{-1}$. For both Model A and Model B, $f_{\text{con},\infty} = 1$ at $f_C \dot{M} \gtrsim 10^{-4} M_\odot \text{ yr}^{-1}$, where the average grain radius scales as $a_{\text{ave},\infty} \propto (f_C \dot{M})^{0.88}$. On the other hand, $a_{\text{ave},\infty}$ is more sensitive to the wind velocity, as seen from Figure 2(b); $a_{\text{ave},\infty}$ is smaller for a higher v_w and scales as $a_{\text{ave},\infty} \propto v_w^{-1.75}$ for $v_w = 1\text{--}100 \text{ km s}^{-1}$. The increase in v_w leads to a lower gas density for a fixed \dot{M} and causes more rapid cooling of the gas, both of which favor producing a number of smaller grains.

The results of the calculations show that the final condensation efficiency of C grains is unity if the following condition is met;

$$\left(\frac{f_C \dot{M}}{3 \times 10^{-3} M_\odot \text{ yr}^{-1}} \right) \left(\frac{v_w}{20 \text{ km s}^{-1}} \right)^{-2} \gtrsim 0.04. \quad (3)$$

Thus, as an example, for $v_w = 20 \text{ km s}^{-1}$ and $f_C = 1$, the total mass of C grains produced over the lifetime of the RSG with $M_{\text{ZAMS}} = 500 M_\odot$ is estimated as $M_{\text{dust}}/M_\odot = 1.7 (\dot{M}/3 \times 10^{-3} M_\odot \text{ yr}^{-1})$ for 1×10^{-4}

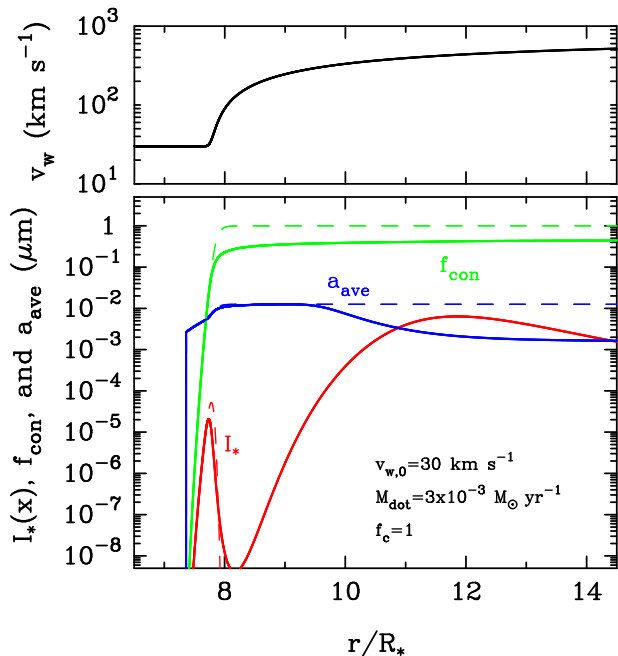


FIG. 3.— Wind velocity v_w (upper panel), and formation rate of seed clusters I_* , condensation efficiency f_{con} , and average grain radius a_{ave} (lower panel) as a function of r/R_* for Model A with the wind acceleration. The initial wind velocity and mass-loss rate are set to be $v_{w,0} = 30 \text{ km s}^{-1}$ and $\dot{M} = 3 \times 10^{-3} M_{\odot} \text{ yr}^{-1}$, respectively. The dashed lines in the lower panel are the results without the wind acceleration.

$M_{\odot} \text{ yr}^{-1} \leq \dot{M} \leq 3 \times 10^{-3} M_{\odot} \text{ yr}^{-1}$. It should be emphasized here that these newly formed grains could not be destroyed by the blast wave resulting from a SN explosion because such a very massive Pop III star would finally collapse into a BH (Heger & Woosley 2002; Yoon et al. 2012, but see also Ohkubo et al. 2006). The ratio of dust mass to the initial stellar mass ($X_{\text{VMS}} = M_{\text{dust}}/M_{\text{ZAMS}} \leq 3.4 \times 10^{-3}$) and the dust-to-metal ratio ($M_{\text{dust}}/M_{\text{metal}} \leq 0.24$) are in the ranges of those supplied by Pop III CCSNe, for which $X_{\text{CCSN}} = (0.1\text{--}30) \times 10^{-3}$ and $M_{\text{dust}}/M_{\text{metal}} = 0.01\text{--}0.25$, depending on the destruction efficiency of newly formed dust by the reverse shocks (Bianchi & Schneider 2007; Nozawa et al. 2007). This implies that, if very massive Pop III stars had really formed, they could be one of rapid and efficient sources of C grains in the early universe.

4. EFFECTS OF WIND ACCELERATION ON DUST FORMATION

In the previous section, we have considered the formation of dust in stellar winds with constant velocities. However, the radiation pressure acting on newly formed grains will drive the wind to higher outflow velocities, which may suppress the growth of the dust grains. Here, according to Ferarroti & Gail (2006), we examine the effect of the wind acceleration on dust formation by solving the following simplified momentum equation:

$$v_w \frac{dv_w}{dr} = -\frac{GM_*}{r^2} \left[1 - \frac{L_* \langle \kappa_{\text{ext}}(T) \rangle}{4\pi c GM_*} D \right], \quad (4)$$

where G is the gravitational constant, c is the light speed, D is the dust-to-gas mass ratio, and $\langle \kappa_{\text{ext}}(T) \rangle$ is the Planck-averaged mass extinction coefficient of C grains.

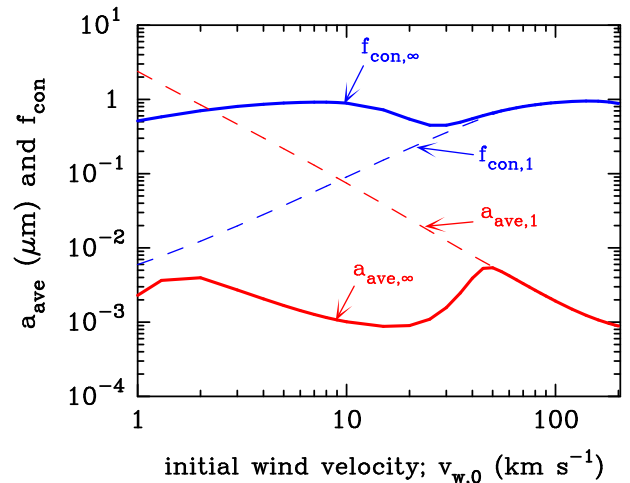


FIG. 4.— The solid lines show the dependence of $a_{\text{ave},\infty}$ and $f_{\text{con},\infty}$ on $v_{w,0}$ in the case with the wind acceleration for Model A with $f_C \dot{M} = 3 \times 10^{-3} M_{\odot} \text{ yr}^{-1}$. The dashed lines plot the average radius $a_{\text{ave},1}$ and condensation efficiency $f_{\text{con},1}$ just before the grain growth is depressed by the wind acceleration.

We take $\langle \kappa_{\text{ext}} \rangle = 2.1 \times 10^4 \text{ cm}^2 \text{ g}^{-1}$ (for $T = 4,440 \text{ K}$, Zubko et al. 1996) and $M_* = 400 M_{\odot}$ as a representative value.

Figure 3 shows the acceleration of the wind and the formation process of dust for the initial outflow velocity of $v_{w,0} = 30 \text{ km s}^{-1}$ and the mass-loss rate of $\dot{M} = 3 \times 10^{-3} M_{\odot} \text{ yr}^{-1}$ in Model A. Because of the high stellar luminosity, the wind is rapidly accelerated to $\geq 100 \text{ km s}^{-1}$ once f_{con} is above $\approx 2 \times 10^{-3}$. The resulting rapid dilution of the gas largely decreases both the growth rate of grains and the formation rate of seed clusters but still allows the dust grains to grow slowly. Furthermore, the expansion of the gas reduces the gas temperature, so very small grains continue condensing from carbon atoms that were not locked up in dust grains, as seen from the later increase in I_* . As a consequence, $a_{\text{ave},\infty}$ becomes very small as a whole, and $f_{\text{con},\infty}$ increases to 0.45.

The dashed lines in Figure 4 plot the average radius ($a_{\text{ave},1}$) and condensation efficiency ($f_{\text{con},1}$) at the time ($t = t_1$) just before the grain growth is suppressed by the wind acceleration, as a function of $v_{w,0}$ for Model A with $f_C \dot{M} = 3 \times 10^{-3} M_{\odot} \text{ yr}^{-1}$. For a lower $v_{w,0}$ with which dust grains form in the region closer to the star, the gas outflow is more efficiently accelerated, and the condensation efficiency of (large) grains formed before the wind acceleration is smaller. Nevertheless, the formation of small grains at later phases, as well as the gradual growth of large grains, enhances $f_{\text{con},\infty}$ up to the range of 0.45–0.95 with the very small $a_{\text{ave},\infty}$ (see the solid lines in Figure 4). Thus, the wind acceleration influences the size distribution of dust but is not likely to affect the final condensation efficiency significantly.

Note that, in these calculations, we consider the acceleration of the winds by assuming the position coupling between the dust and the gas. In reality, dust grains pushed by the radiation pressure move outwards relative to the gas, then the drag force between them drives the acceleration of the outflowing gas. Thus, the wind acceleration must be less efficient than that in this study. On the other hand, the high-velocity motion of dust relative to the gas can cause the erosion of dust by sputtering

(Tielens et al. 1994; Nozawa et al. 2006). In particular, dust grains are accelerated above 100 km s^{-1} in the present case, so the processing of dust by sputtering is expected to have considerable impacts on the final condensation efficiency. These processes will be explored in the future work.

5. CONCLUSION AND DISCUSSION

We have investigated the formation of C grains in a mass-loss wind of a Pop III RSG with $M_{\text{ZAMS}} = 500 M_{\odot}$. We find that, in a stellar wind with a constant velocity, the condensation efficiency of C grains is unity under the condition in Equation (3), and that at most $1.7 M_{\odot}$ of C grains can be produced during the lifetimes of Pop III RSGs. We also find that the wind acceleration caused by newly formed dust can change the final size distribution of the dust, but still leads to the high final condensation efficiency ($f_{\text{con},\infty} \gtrsim 0.5$). Such dust masses would be high enough to have an impact on the dust enrichment history in the early universe if the IMF of Pop III stars was top-heavy.

Recent sophisticated simulations of the first star formation (Hirano et al. 2014) have suggested that the number of very massive stars (VMSs) with $M_{\text{ZAMS}} \gtrsim 250 M_{\odot}$ (N_{VMS}) is likely to be as large as that of massive stars exploding as CCSNe (N_{CCSN}). If this is true and if all of the VMSs lead to $X_{\text{VMS}} = 3.4 \times 10^{-3}$, the contribution of the interstellar dust from VMSs is comparable with, or even higher ($N_{\text{VMS}}X_{\text{VMS}}/N_{\text{CCSN}}X_{\text{CCSN}} \gtrsim 1$) than that from CCSNe in the case that the destruction of dust by the reverse shock is efficient ($X_{\text{CCSN}} \lesssim 1.0 \times 10^{-3}$).⁹ Thus, very massive Pop III stars could be potentially dominant sources of dust grains at very early times of the universe.

Our results also have important indications on the formation scenario of carbon-rich ultra-metal-poor (UMP) stars with $[\text{Fe}/\text{H}] < -4$, which would record the chemical imprints of Pop III stars (Beers & Christlieb 2005). The formation of such low-mass metal-poor stars is considered to be triggered through the cooling of gas by dust ejected from Pop III SNe (Schneider et al. 2012a, 2012b; Chiaki et al. 2013). Ji et al. (2014) suggested that the formation of carbon-rich UMP stars relies on the cooling by fine structure lines of C and O atoms, assuming that the first SNe produced no C grain.

Here we propose another possible channel for the formation of carbon-rich UMP stars. As shown in this study, very massive Pop III RSGs are efficient sources of C grains as well as CNO elements. Thus, in the gas clouds enriched by these Pop III RSGs, C grains enable the formation of low-mass stars whose chemical compositions are highly enhanced in carbon and oxygen. As the investigated $500 M_{\odot}$ model undergoes mild hot-bottom burning, some nitrogen is also produced, giving rise to $[\text{N}/\text{C}] = -4.2$ to -1.3 depending on the assumed mass-loss history, where observations of carbon-rich UMP stars indicate $[\text{N}/\text{C}] \geq -1.7$ (Christlieb et al. 2002; Norris et al. 2007; Frebel et al. 2008). From our zero-metallicity model, we do not predict the presence of any heavier

metals. Further observations and more quantitative theoretical studies are needed to show whether any UMP stars have formed through our scenario.

We are grateful to the anonymous referees for critical comments. This research has been supported by World Premier International Research Center Initiative (WPI Initiative), MEXT, Japan, and by the Grant-in-Aid for JSPS Scientific Research (22684004, 23224004, 23540262, 26400222).

⁹ For pair-instability SNe occurring from stars with $M_{\text{ZAMS}} \simeq 130\text{--}250 M_{\odot}$, $X_{\text{PISN}} \lesssim 0.05$ and $M_{\text{dust}}/M_{\text{metal}} \lesssim 0.15$, depending on the destruction efficiency of dust by the reverse shocks (Nozawa et al. 2007). We also note that pair-instability SNe might be inefficient sources of C grains (Nozawa et al. 2003).

REFERENCES

- Beers, T. C., & Christlieb, N. 2005, *ARA&A*, 43, 531
- Bertoldi, F., Carilli, C. L., Cox, P., et al. 2003, *A&A*, 406, L55
- Bianchi, S., & Schneider, R. 2007, *MNRAS*, 378, 973
- Bromm, V., & Larson, R. B. 2004, *ARA&A*, 42, 79
- Chase, M. W. Jr., Davies, C. A., Downey, J. R. Jr., et al., 1985, *JANAF Thermochemical Tables*, 3rd ed. *J. Phys. Chem. Ref. Data*, 14, Suppl. 1
- Chiaki, G., Nozawa, T., & Yoshida, N. 2013, *ApJ*, 765, L3
- Christlieb, N., Bessell, M. S., Beers, T. C., et al. 2002, *Nature*, 419, 904
- Dwek, E., Galliano, F., & Jones, A. P. 2007, *ApJ*, 662, 927
- Dwek, E., & Cherchneff, I. 2011, *ApJ*, 727, 63
- Ferrarotti, A. S., & Gail, H.-P. 2006, *A&A*, 447, 553
- Frebel, A., Collet, R., Eriksson, K., Christlieb, N., & Aoki, W. 2008, *ApJ*, 684, 588
- Gail, H.-P., Keller, R., & Sedlmayr, E. 1984, *A&A*, 133, 320
- Gall, K., Andersen, A. J., & Hjorth, J. 2011a, *A&A*, 528, A13
- Gall, K., Andersen, A. J., & Hjorth, J. 2011b, *A&A*, 528, A14
- Heger, A., & Woosley, S. E. 2002, *ApJ*, 567, 532
- Hirano, S., Hosokawa, T., Yoshida, N., et al. 2014, *ApJ*, 781, 60
- Hosokawa, T., Omukai, K., Yoshida, N., & Yorke, H. W. 2011, *Science*, 334, 1250
- Kochanek, C. S. 2014, submitted to *MNRAS* (arXiv:1402.4812)
- Ji, A. P., Frebel, A., & Bromm, V. 2014, *ApJ*, 782, 95
- Kozasa, T., Dorschner, J., Henning, Th., & Stognienko, R. 1996, *A&A*, 307, 551
- Norris, J. E., Christlieb, N., Korn, A. J., et al. 2007, *ApJ*, 670, 774
- Nozawa, T., & Kozasa, T. 2013, *ApJ*, 776, 24
- Nozawa, T., Kozasa, T., Habe, A. 2006, *ApJ*, 648, 435
- Nozawa, T., Kozasa, T., Habe, A., et al. 2007, *ApJ*, 666, 955
- Nozawa, T., Kozasa, T., Umeda, H., Maeda, K., & Nomoto, K. 2003, *ApJ*, 598, 785
- Ohkubo, T., Nomoto, K., Umeda, H., Yoshida, N., & Tsuruta, S. 2009, *ApJ*, 706, 1184
- Ohkubo, T., Umeda, H., Maeda, K., et al. 2006, *ApJ*, 645, 1352
- Omukai, K., & Palla, F. 2003, *ApJ*, 589, 677
- Priddey, R. S., Isaak, K. G., McMahon, R. G., Robson, E. I., & Pearson, C. P. 2003, *MNRAS*, 344, L74
- Schneider, R., Omukai, K., Bianchi, S., & Valiante, R. 2012a, *MNRAS*, 419, 1566
- Schneider, R., Omukai, K., Limongi, M., et al. 2012b, *MNRAS*, 423, L60
- Susa, H. 2013, *ApJ*, 773, 185
- Tielens, A. G. G. M., McKee, C. F., Seab, C. G., & Hollenbach, D. J. 1994, *ApJ*, 431, 321
- Valiante, R., Schneider, R., Bianchi, S., & Andersen, A. C. 2009, *MNRAS*, 397, 1661
- Valiante, R., Schneider, R., Salvadori, S., & Bianchi, S. 2011, *MNRAS*, 416, 1916
- Yoon, S.-C., Dierks, A., & Langer, N. 2012, *A&A*, 542, A113
- Zhang, W., Woosley, S. E., & Heger, A. 2008, *ApJ*, 679, 639
- Zubko, V. G., Mennella, V., Colangeli, L., & Bussoletti, E. 1996, *MNRAS*, 282, 1321